O 2p holes: Temperature effects and surface characteristics of cuprate superconductors

T. J. Wagener, H. M. Meyer III, Yongjun Hu, M. B. Jost, and J. H. Weaver
Department of Chemical Engineering and Materials Science, University of Minnesota, Minneapolis, Minnesota 55455

K. C. Goretta
Argonne National Laboratory, Argonne, Illinois 60439
(Received 15 September 1989)

The O 2p holes in the Cu- and Bi-based oxide superconductors La-Sr-Cu-O, Y-Ba-Cu-O, Bi-Sr-Ca-Cu-O, Tl-Ba-Ca-Cu-O, and Ba-K-Bi-O, and in CuO have been investigated with inverse photoelectron spectroscopy. These states exhibit a unique resonance for incident electron energies near the O 2s shallow core in the Cu-based superconductors but it is not observed in CuO or in Ba-K-Bi-O. Variations in the resonance show that the number of O 2p holes (1) increases at 60 K compared to 300 K, (2) is significantly reduced in oxygen-deficient samples, (3) is altered but not quenched upon Pr substitution for Y, (4) is reduced by electron bombardment at ~1500 eV, and (5) is quenched by Cu- or Au-adatom-induced surface disruption. The Bi-Sr-Ca-Cu-O surfaces are found to be the most stable against high-energy electron bombardment and interface formation.

INTRODUCTION

Recent interest in the high-T_c superconductors has centered on the O 2p holes since they are believed to play an active role in this novel phenomenon.[1-5] In particular, Hall-effect studies have shown holes to be the majority charge carriers in the normal state,[6,7] and optical absorption[8-12] and electron-energy-loss-spectroscopy (EELS)[13-17] measurements have shown O 2p holes near the Fermi level E_F. By applying dipole selection rules, it was determined that these O 2p holes have $p_{x,y}$ character with x,y in the a-b plane.[12,14,16] The absence of O 2p holes has been reported for O-deficient $YBa_2Cu_3O_{7-x}$ and undoped La_2CuO_4 cuprates.[10,15] On the other hand, their presence has been documented in nonsuperconducting $PrBa_2Cu_3O_{6,8}$ (Ref. 17) and $EuBa_2(Cu_{1-y}Zn_y)_3O_7$ (Ref. 11). Direct observation and energy placement of these holes has been accomplished with inverse photoelectron spectroscopy (IPES),[18-20] taking advantage of resonant enhancement of O 2p states that occurs near the O 2s threshold.[21] Of particular interest here is the nature of this O 2p hole resonance and how it changes with temperature. We are also interested in O 2p variation among the high-T_c superconductors and related compounds, and how changes in surface or bulk characteristics affect it.

In this paper, we present results of a detailed investigation of the unoccupied electronic states of the oxide superconductors $La_{1.85}Sr_{0.15}CuO_4$, (La-Sr-Cu-O), $YBa_2Cu_3O_{7-x}$ (Y-Ba-Cu-O), $Bi_2Sr_2Ca_{0.8}Y_{0.2}Cu_2O_{8+y}$ (Bi-Sr-Ca-Cu-O), $Tl_2Ba_2Ca_2Cu_3O_{10+y}$ (Tl-Ba-Ca-Cu-O), and $Ba_{1-x}K_xBiO_{3-y}$ (Ba-K-Bi-O), paying particular attention to the states near E_F. As a reference compound, we have studied CuO. Incident-electron energy-dependent studies of CuO and Ba-K-Bi-O at the O 2s threshold show no O 2p empty-state enhancement, but enhancement is found for all of the cuprate superconductors. Temperature-dependent studies of Y-Ba-Cu-O and Bi-Sr-Ca-Cu-O reveal greater O 2p hole emission at 60 K than at 300 K, and we propose that there is enhanced charge transfer from O to Cu at lower temperatures. Equivalent studies of nonsuperconducting $YBa_2Cu_3O_{6.25}$ and $PrBa_2Cu_3O_{7-x}$ show these empty O 2p holes drastically reduced and altered. Finally, we examine changes in surface character caused by high-energy electron bombardment and Cu and Au adatom deposition, finding that the Bi-Sr-Ca-Cu-O surface is affected less than Y-Ba-Cu-O.

EXPERIMENTAL

IPES studies were conducted in a four-chamber ultra-high-vacuum system (pressure $<1\times10^{-10}$ Torr) optimized for photon detection at ultraviolet and x-ray energies ($h\nu=10$–44 and 1486.6 eV).[22] A 1×5-mm^2 monoenergetic sheet beam of electrons was focused onto the sample by a Pierce-type electron gun manufactured by Kimball physics. Typical beam currents were ~10 μA at low energies and ~100 μA at x-ray energies. The emitted ultraviolet photons were dispersed by a grating monochromator onto a position sensitive detector (total energy resolution 0.3 eV at $h\nu=10$ eV and 1 eV at $h\nu=44$ eV). A crystal monochromator was used to select photons of energy 1486.6 eV and direct them onto a chevron channel plate detector (resolution ~0.7 eV). The energy zero, E_F, was determined from the emission onset of metallic Pd in electrical contact with the sample. Low temperatures were achieved by connecting the samples to a closed cycle helium refrigerator via a copper braid. A Au–0.07 at. % Fe versus Chromel thermocouple was used to monitor temperature. Clean surfaces could be prepared at 60 and 300 K, and changes upon warming or cooling could be monitored.

Preparation of our polycrystalline superconducting cuprates and Ba-K-Bi-O has been described previously.[23,24] Resistance measurements showed superconducting tran-

sition temperatures, taken as the midpoint of the transition, of 35 K for La-Sr-Cu-O, 93 K for Y-Ba-Cu-O, 85 K for Bi-Sr-Ca-Cu-O, 118 K for Tl-Ba-Ca-Cu-O, and 27 K for Ba-K-Bi-O. Precut posts were then fractured *in situ*. Parallel studies using x-ray photoelectron spectroscopy (XPS) showed surfaces prepared in this way to have a single O 1*s* core level centered at ~529 eV, with a shoulder at ~531 eV. The 531-eV feature is a well-known signature of grain boundary phases in these cuprate superconductors.[25]

The nonsuperconducting $YBa_2Cu_3O_{6.25}$ samples were synthesized from reagent grade Y_2O_3, $BaCO_3$, and CuO.[26] The reaction was carried out at 800 °C in O_2 of reduced total pressure.[27,28] The resultant powder was pressed into pellets and sintered for 2.5 h in air at 950 °C. Equilibrium oxygen content was taken from the data of Gallagher[29] and Kishio *et al.*[30] The $PrBa_2Cu_3O_{7-x}$ samples were synthesized from reagent grade $PrO_{1.818}$, $BaCO_3$, and CuO. Pressed pellets of $PrBa_2Cu_3O_{7-x}$ were sintered at 960 °C for 2 h, followed by annealing in O_2 at 425 °C.

Samples of CuO were prepared by resistively heating a Cu foil to 900 °C, followed by cooling in oxygen at atmospheric pressure. The resulting CuO films had a thickness of ~1 μm, thick enough to represent a bulk sample yet thin enough to avoid charging. After synthesis, they were transferred to the measurement chamber and were sputtered with 500-eV Ar^+ atoms. Auger electron spectroscopy showed the sputtered surface to be free of contaminants with an oxygen to copper signal ratio indicative of CuO.

RESULTS AND DISCUSSIONS

Energy dependent IPES studies of CuO

Recent interest in copper monoxide, CuO, stems from the discovery of the cuprate superconductors.[31,32] In CuO, the Cu atoms are at the center of slightly distorted oxygen rectangles, with distance to the four O atoms of ~1.95Å.[33] For the superconducting perovskites, Cu is fourfold with oxygen in the *a-b* plane and the nearest neighbor distance is ~1.9 Å.

Studies of CuO have emphasized the effects of electron correlation on the electronic structure. Band-structure calculations predict CuO to be metallic,[31,32] but experiment shows it to be an antiferromagnetic semiconductor with a band gap of ~1.4 eV.[34] For CuO, the Cu ground-state electronic configuration can be written as a mixture of d^9 and $d^{10}\underline{L}$, where $\underline{L}$ denotes a suitably symmetrized hole on the oxygen ligand.[35] With this in mind, the photoemission final state becomes a mixture of d^8, $d^9\underline{L}$, and $d^{10}\underline{L}^2$ configurations. Photoemission results show the d^8 satellite features near 10 and 12.4 eV below E_F,[31,35] shifted from the one-electron energy level by the Coulomb *d-d* repulsive interaction of two holes in the Cu *d* shell.[31] The $d^9\underline{L}$ levels lie predominantly between 1 and 5 eV, somewhat broadened and shifted to higher binding energy relative to their one-electron energies predicted by band calculations.[31]

In Fig. 1 we show the distribution of empty states via photon distribution curves (PDC's) for CuO. The spectra are aligned to the conduction-band minimum, E_c, which lies within 0.1 eV of the spectrometer Fermi level. The top curve was obtained from bremsstrahlung isochromat spectroscopy (BIS) measurements at $h\nu = 1486.6$ eV as the incident electron energy was scanned between 1484 and 1506 eV. The lower curves were taken for incident electron energies, $15 \leq E_i \leq 35$ eV, as labeled. In all cases E_i is referenced to E_F.

The IPES spectra for CuO in Fig. 1 are of particular interest since empty-state structures that indicate O 2*p* and Cu 3*d* features should have very different emission intensities in this energy range.[36] In particular, the Cu 3*d*/O 2*p* emission ratio increases from 0.7 for $E_i = 15$ eV to 1.2 for $E_i = 35$ eV and 60 for 1486.6 eV.[37] Indeed, the distinct shoulder ~1 eV above E_c for lower E_i's becomes

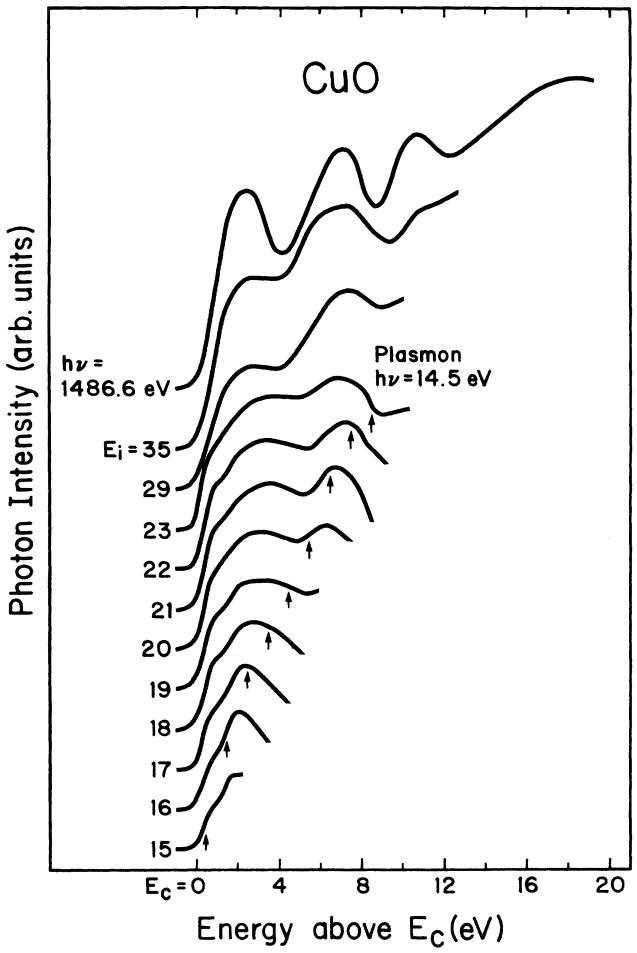

FIG. 1. Unoccupied electronic states of CuO from the conduction-band minimum E_c to $E_F + 25$ eV. The top curve was acquired in the BIS mode at $h\nu = 1486.6$ eV, while the others were acquired at constant incident electron energies E_i, as labeled. The shoulder at 1 eV above E_c corresponds to unoccupied O 2*p* states, while that at 2.4 eV reflects Cu $3d^{10}$ final-state character. Arrows indicate where plasmon energy losses occur, although their effects are weak in this range of incident electron energies.

negligible by $E_i = 35$ eV, and we attribute it to unoccupied O $2p$ levels. This is supported by localized augmented-spherical-wave (LASW) calculations that predicted that O $2p$ levels lie close to E_F.[31,32] Furthermore, x-ray absorption studies involving O $1s$ electrons show O $2p$ levels ~ 1 eV above E_c.[32]

Our BIS spectrum in Fig. 1 shows an unoccupied-state feature 2.4 eV above E_c, in agreement with that presented by Ghijsen *et al.*[31] As those authors noted, this feature is due to the completion of the Cu $3d$ shell, i.e., the $3d^{10}$ final state achieved by electron capture. Photoionization cross-section considerations support this interpretation since Cu $3d$ features are expected to be more pronounced at x-ray energies, as observed.

Figure 1 shows structures centered ~ 7, 10.8, and 18 eV above E_c that remain constant in energy but are modulated in intensity with E_i. LASW calculations predict Cu- and O-derived levels near 7, 10, and 18 eV.[31,32] Comparison of theory and experiment is quite good for the higher-lying levels, yet disagreement is found for the unoccupied Cu $3d$ levels at 2.4 eV and O $2p$ levels at ~ 1 eV. We find that the experimentally-determined Cu $3d^{10}$ level lies ~ 1 eV further from E_c than the d states obtained for one-electron calculations. Ghijsen *et al.*[31] found and discussed a similar difference between their ground-state calculations the experimental final state. In a local picture, the addition of one electron formally converts the CuO d^9 and $d^{10}\underline{L}$ ground states to d^{10} and $d^{10}L$ final states. Since L represents a filled ligand, these two final states are identical, and only one Cu d feature is observed. This is in contrast to the picture for NiO where the ground state is a mixture of d^8 and $d^9\underline{L}$ and becomes d^9 and $d^{10}\underline{L}$ in the IPES final state. Indeed, BIS results show two different final states for IPES studies of NiO corresponding to the d^9 feature ~ 1.8 eV above E_F and the $d^{10}\underline{L}$ satellite feature ~ 18 eV above E_F.[38]

The spectra in Fig. 1 show that emission ~ 1 eV above E_c increases continuously with E_i. Of particular importance is the emission intensity of the O $2p$ states as E_i is increased from 15 to 35 eV. Previously we have shown that there is an enhancement that occurs at $E_i \sim 18$ eV because of the O $2s$-$2p$ resonance. To examine this effect for CuO we can plot the intensity at a fixed final state as a function of E_i to obtain inverse constant-final-state (ICFS) spectra (see Refs. 18 and 19). ICFS curves for CuO taken for final states 1 eV above E_F show a constant increase with E_i, with no structure that can be associated with the O $2s$ threshold energy. Recalling that the relative photoionization cross section of the Cu $3d$ levels increases in this region, we attribute this growth to the presence of the Cu $3d$ levels 2.4 eV above E_c. The absence of resonant enhancement of the unoccupied $2p$ levels in CuO is probably because the O-derived states are very highly hybrized.

The arrows in Fig. 1 show where contributions due to radiative plasmon decay occur. These features are observed with IPES because incident electrons can excite plasmons that radiatively decay and emit constant energy photons. Since the IPES spectra are aligned at E_F, the plasmon feature at $h\nu = 14.5$ eV moves to the right with increasing E_i. This radiative decay channel is quite small for the range of E_i in Fig. 1 and is easier to distinguish at higher E_i because it no longer overlaps direct decay channels involving conduction-band states. Similar plasmon loss features have been observed for many materials,[39] including the cuprate superconductors.[18,19] They appear at $h\nu = 13.3$ eV for La-Sr-Cu-O, 22.2 eV for Y-Ba-Cu-O, 21.2 and 15 eV for Bi-Sr-Ca-Cu-O, and 20.2 and 12.5 eV for Tl-Ba-Ca-Cu-O.[18,19]

Comparison of CuO and Cu-O based superconductors

The results of Fig. 1 for CuO provide a basis for examining the empty states of the CuO-derived superconductors, particularly states that lie near E_F. In Fig. 2 we present room-temperature IPES spectra between E_F and $E_F + 3$ eV for La-Sr-Cu-O, Y-Ba-Cu-O, Bi-Sr-Ca-Cu-O, Tl-Ba-Ca-Cu-O, Ba-K-Bi-O, and CuO. (Figure 2 shows results for Y-doped Bi-Sr-Ca-Cu-O, but equivalent results were obtained for the parent material.[18]) These spectra are representative of on-resonance ($E_i = 17$ or 18 eV) and off-resonance ($E_i = 15$, 16, or 20 eV) for O $2s$-$2p$ excitations, and the dashed curve represents the difference. In

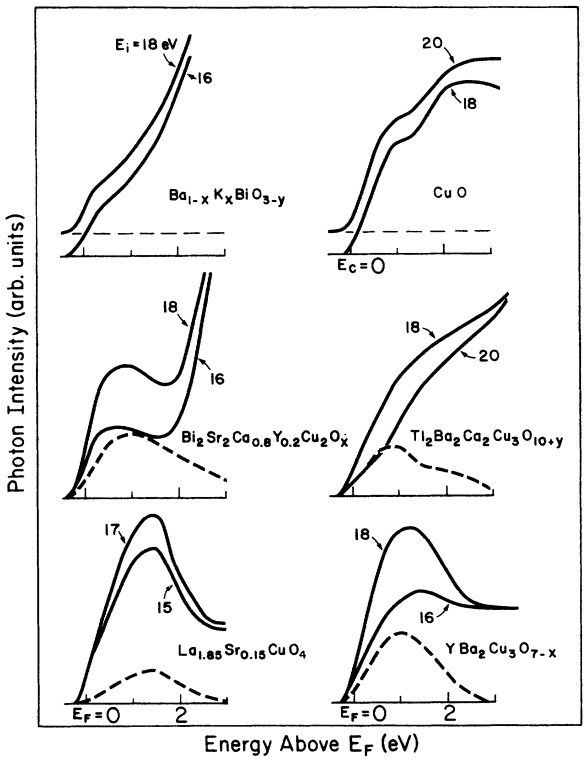

FIG. 2. Room temperature IPES spectra to $E_F + 3$ eV for La-Sr-Cu-O, Y-Ba-Cu-O, Bi-Sr-Ca-Cu-O, Tl-Ba-Ca-Cu-O, Ba-K-Bi-O, and CuO. Solid curves correspond to excitations at and above or below the O $2s$-$2p$ resonance. The four cuprate superconductors all exhibit the O $2p$ hole state resonance at ~ 18 eV, while Ba-K-Bi-O and CuO do not. Difference curves (dashed lines) represent the states enhanced by the O $2s$-$2p$ transition, with similar distributions found for *all* cuprate superconductors.

each case, the results have been normalized to electron dose. While they therefore are quantitative for any given compound, there is no unique normalization procedure among the different compounds. The overall experimental resolution at $E_i = 18$ eV is 0.4 eV.

The four cuprate superconductors and Ba-K-Bi-O exhibit a distinct Fermi-level cutoff, although the emission is low and the presence of structure at ~ 1 eV makes the leading edges appear broadened. One-electron band-structure calculations[40] suggest that the states at E_F for the cuprate superconductors have Cu $3d_{x^2-y^2}$–O $2p_{x,y}$ character, with additional Bi p and O p hybrids and Tl-O sp hybrid states for Bi-Sr-Ca-Cu-O and Tl-Ba-Ca-Cu-O, respectively. Ba-K-Bi-O is expected to have hybrid states of Bi s and O $2p$ character at E_F.[41] The results of Fig. 1 for CuO showed a Cu $3d^{10}$ peak at $E_c + 2.4$ eV, but no such obvious feature appears for any of the cuprates shown in Fig. 2. By performing BIS measurements on Y-Ba-Cu-O, we hoped to enhance the Cu $3d^{10}$ cross section and gain insight into its energy location and character, but the results were inconclusive because of electron-induced surface damage, as will be discussed later.

The results of Fig. 2 clearly show enhancement for $E_i \sim 18$ eV for all of the Cu-O based superconductors. In contrast, there is no enhancement for Ba-K-Bi-O or CuO (the on- and off-resonance spectra for them have been offset to show that they are nearly identical). Since this enhancement does not occur at a constant photon energy, any process that requires a constant photon energy can be ruled out, including plasmons,[39] direct core-hole recombination, or luminescence.[42] It is unlikely that this enhancement is caused by a van Hove singularity in the joint density of states[43] since IPES studies of single-crystal Y-Ba-Cu-O (Ref. 44) show the emission between E_F and $E_F + 2$ eV changes with incident electron angle because of band-structure effects but the relative emission for $E_i = 16$ and 18 eV remains constant. Thus, the ratio of the areas under the $E_i = 16$- and 18-eV IPES spectra between E_F and $E_F + 2$ eV is independent of angle and is approximately equal to that found for our polycrystalline Y-Ba-Cu-O samples. Finally, detailed ICFS curves taken with $E_f = 1$ eV for both Y-Ba-Cu-O and Bi-Sr-Ca-Cu-O are consistent with a Fano-type resonance process.[45]

We attribute the increased emission between E_F and $E_F + 2$ eV at $E_i = 18$ eV to the resonant enhancement of the O $2p$ holes via the O $2s$ shallow core level. The incident electron induces an O $2s$ core excitation into unoccupied O $2p$ levels. Radiative decay channels of the core hole,

$$\mathrm{O}(2s^1 2p^6) \rightarrow \mathrm{O}(2s^2 2p^5) + h\nu \ ,$$

couple with the IPES decay continuum and produce resonant enhancement.[21] The fact that resonance is not observed for Ba-K-Bi-O, which is a high-temperature superconductor with O $2p$ holes, or CuO, which has empty $2p$ states, suggests a unique O bonding configuration in the planar CuO-based superconductors.

There exists a ~ 3-eV discrepancy between the observed energy of the O $2s$-$2p$ resonance and the expected energy based on one-electron energies. Photoemission results consistently place the centroid of the O $2s$ levels ~ 20 eV below E_F,[19] while IPES results place the center of the unoccupied O $2p$ levels at 1 eV above E_F. Within a one-electron picture, one would expect the resonant energy to occur near 21 eV, rather than 18 eV as we observed for *all* of the cuprate superconductors. Photoemission results by Takahashi *et al.*[46] also show enhancement at $h\nu = 18$ eV of the occupied O $2p$ states between $E_F - 1$ eV and E_F. Wendin[21] has suggested that this may be because of an asymmetry towards lower binding energy of the O $2s$ shallow core level corresponding to a "well screened" O $2s2p^6$ configuration.

The difference curves shown in Fig. 2 are remarkably similar to each other, showing a peak at $E_F + 1$ eV with full width of half maximum (FWHM) of ~ 1.5 eV. For La-Sr-Cu-O and Y-Ba-Cu-O, the shape of the difference curves resembles the PDC's themselves between E_F and $E_F + 2$ eV, a result expected based upon one-electron band theory since there are only Cu-O states near E_F for these two compounds.[40] On the other hand, the difference curves and the regular IPES spectra for Bi-Sr-Ca-Cu-O and Tl-Ba-Ca-Cu-O are quite different, and we attribute this to the presence of Bi-O and Tl-O hybrid or-

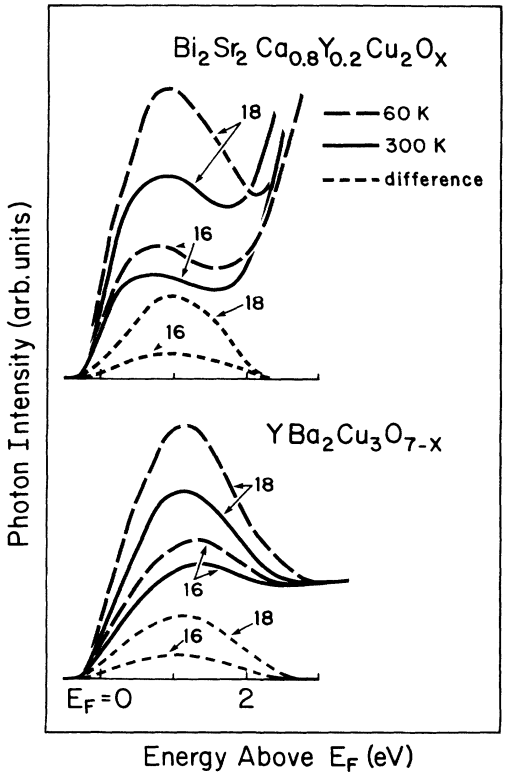

FIG. 3. IPES spectra for Y-Ba-Cu-O and Bi-Sr-Ca-Cu-O acquired at 300 K (solid lines) and 60 K (dashed lines). The surfaces were fractured at the measurement temperature. The lower curves were acquired off the O $2s$-$2p$ resonance ($E_i = 16$ eV), while the upper curves were taken at resonance ($E_i = 18$ eV). We find increased O $2p$ hole emission at 60 K. The dotted curves represent differences in the 16- and 18-eV spectra resulting from the temperature change.

bitals.[40] We conclude that these hole states are similar for all of the cuprate superconductors, a conclusion also reached by photoemission for the occupied Cu-O hybrid manifold.[23]

Temperature effects and surface variation

Several photoemission studies have focused on changes in the electronic structure of the high-T_c superconductors induced by temperature. High-resolution results have successfully observed the opening of the superconducting gap for Y-Ba-Cu-O and Bi-Sr-Ca-Cu-O.[47–49] To investigate temperature-induced effects in the empty states, we undertook IPES studies of Y-Ba-Cu-O and Bi-Sr-Ca-Cu-O at 60 and 300 K. While the resolution of IPES is far from being able to see a gap develop, it was thought that changes in the O 2p features might be observed and such effects would be critical for understanding the hole population. In these studies, the samples were fractured at 60 or 300 K. Parallel XPS studies at 20 and 300 K showed negligible contamination as determined by the O 1s relative magnitude of the feature located at ~531 eV. We found no evidence for oxygen loss or surface instability.

In Fig. 3 we compare spectra for Y-Ba-Cu-O and Bi-Sr-Ca-Cu-O taken at 60 K (dashed curves) and 300 K (solid curves). The spectra were acquired within 30 min of fracture and were normalized to constant photon emission height at E_F+3 eV for Y-Ba-Cu-O and E_F+4 eV for Bi-Sr-Ca-Cu-O (the samples were electrically grounded in these temperature-dependent studies and the electron dose could not be measured). This normalization procedure gave nearly identical results to that of Fig. 2 for the 300 K studies. The dotted curves represent differences resulting from temperature changes in the 16- and 18-eV spectra.

The spectra in Fig. 3 show an increase in photon emission intensity between E_F and E_F+3 eV for 60 K compared to 300 K for both Y-Ba-Cu-O and Bi-Sr-Ca-Cu-O. Comparison of the difference curves (dotted lines) obtained for $E_i=16$ and 18 eV reveals a greater temperature-induced change for spectra taken on resonance at $E_i=18$ eV than off resonance at 16 eV. Moreover, the difference spectra arising from the temperature effects closely resembles those in Fig. 2, where resonance photoemission was used to highlight the O 2p character of the empty states. Finally, the resonant enhancement at 60 K is ~10% greater than the resonant enhancement at 300 K for both Y-Ba-Cu-O and Bi-Sr-Ca-Cu-O. We conclude that the increased emission at low temperature is because of an increase in the number of O 2p hole states; the enhanced emission at $E_i=18$ eV reflects their resonant behavior.

For Y-Ba-Cu-O, the increased emission from the O 2p holes at 60 K occurs with no other significant changes in the unoccupied electronic structure, including the position and width of the corelike Ba 4f level.[50] Our XPS studies also show no changes in the occupied Y and Ba core levels as a function of temperature. However, the XPS results do show a decrease in the Cu^{2+} $2p_{3/2}$ satellite emission at 20 K compared to 300 K, along with line-shape changes in the O 1s core-level emission (no changes were found in the weak ~531 eV component). Sarma *et al.*[51] observed similar changes in the Cu^{2+} $2p_{3/2}$ satellite emission upon cooling. We conclude that these significant temperature effects are associated with the CuO_2 planes. We suggest that the increase in O 2p holes at 60 K is a consequence of greater amounts of charge transfer from O to Cu in the CuO_2 planes.

To further investigate the temperature dependence of the empty states, we cooled to 60 K a sample of Y-Ba-Cu-O fractured at 300 K. Upon cooling, we found enhanced emission ~1.0 eV above E_F with FWHM of ~1.5 eV. The character of this enhancement is identical to the difference curves shown in Figs. 2 and 3, again suggesting that the changes are because of an increased number of O 2p holes.[52] After these measurements, the sample was warmed from 60 to 300 K, but the results were inconclusive because of contamination resulting from pressure bursts ($<1\times10^{-9}$ Torr) associated with warming of the Cu braid and sample holder. Equivalent XPS results show significant increases in the O 1s 531-eV contamination feature and changes in the valence band when a sample is warmed from 20 to 300 K. Such changes can be attributed to chemical modification of the surface region without postulating the loss of O from the superconductor.

In Fig. 4 we show IPES spectra taken at $E_i=18$ eV as a sample of Bi-Sr-Ca-Cu-O was cooled from 300 to 60 K (temperature uncertainty ±5 K). The dashed curves were acquired at 300 K. The difference curves shown at the right show increased O 2p hole emission at lower temperature. The spectra at the left also show changes at ~2.8 eV, which could be viewed either as a shift in the curve or a loss in emission at 2.8 eV. The difference curves at the right show that the effect grows with decreasing tempera-

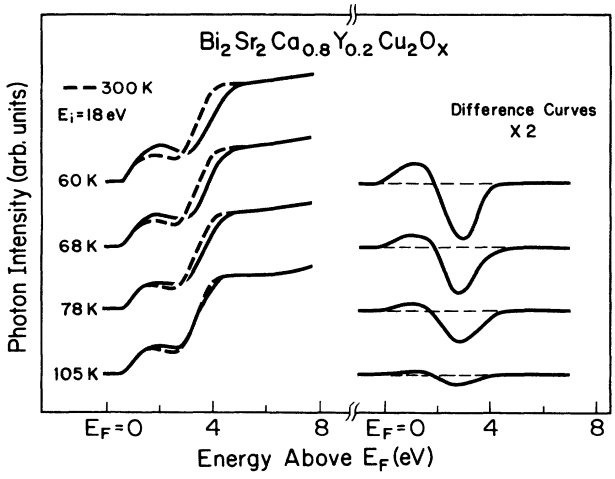

FIG. 4. IPES spectra representing the effects of cooling a 300-K fractured Bi-Sr-Ca-Cu-O sample to 60 K. On the left, we compare the spectra for a sample fractured at 300 K (dashed line) taken at $E_i=18$ eV with those acquired at the lower temperature (solid lines). Difference curves on the right show a progressive increase in the amount of emission because of the O 2p holes and decrease in the Cu 3d emission upon cooling.

ture (maximum at 2.8 eV, FWHM=1.2 eV). Since our temperature dependent XPS studies of Bi-Sr-Ca-Cu-O showed no changes in binding energy for the occupied Bi $4f$ or $5d$ levels, we can discount the possibility of a shift in the Bi $5p$ feature at $\sim E_F+4$ eV. Spectra acquired at $E_i=16$ and 18 eV showed no changes that would suggest that the 2.8-eV feature is associated with O $2p$ levels.

We propose that the feature at $E_F+2.8$ eV is associated with the unoccupied Cu $3d$ levels of Bi-Sr-Ca-Cu-O. We note that IPES results by Drube *et al.*[20] showed a sharp feature 2.9 eV above E_F, the magnitude of which was cleave dependent. At that time, it was unclear whether it was because of a localized $3d$ final-state feature or was part of the Bi-O hybrid manifold. Given the present evidence for enhanced charge transfer at low temperature for Y-Ba-Cu-O and evidence for increased O $2p$ hole population at 60 K for Bi-Sr-Ca-Cu-O, we favor the association of the 2.8 feature with Cu d character. The reduction of that structure at low temperature again reflects a net charge transfer involving Cu and O, thus increasing the O $2p$ hole density and favoring the Cu $3d^{10}$ initial-state configuration at low T (i.e., changing from Cu^{2+} to Cu^{1+} ground state).

The results of Fig. 4 show spectral changes associated with unoccupied O $2p$ and Cu $3d$ features that begin at ~ 105 K and increase to at least 60 K. These results are summarized in Fig. 5, where the amount of change in the O $2p$ (open circles) and Cu $3d$ (solid circles) features are plotted as a function of temperature. While the error bars are rather large, there is a clear trend that shows an increase in O $2p$ emission and a decrease in the Cu $3d$ levels upon cooling, and these changes occur near T_c. Upon warming, emission at 2.8 eV reappears, i.e., the process is reversible.

Finally, we note that the amount of O $2p$ emission was smaller for Y-Ba-Cu-O samples fractured at 300 K and cooled to 60 K than for those fractured and measured at 60 K. For Bi-Sr-Ca-Cu-O, however, the same $2p$ emission was observed at 60 K, regardless of whether the sample was prepared at 60 or 300 K, perhaps because Bi-Sr-Ca-Cu-O fractures between the Bi-O planes,[53] resulting in more stable surfaces. Results obtained following high-energy electron bombardment and adatom deposition show that the O $2p$ hole emission is very susceptible to structural disruption, particularly for Y-Ba-Cu-O.

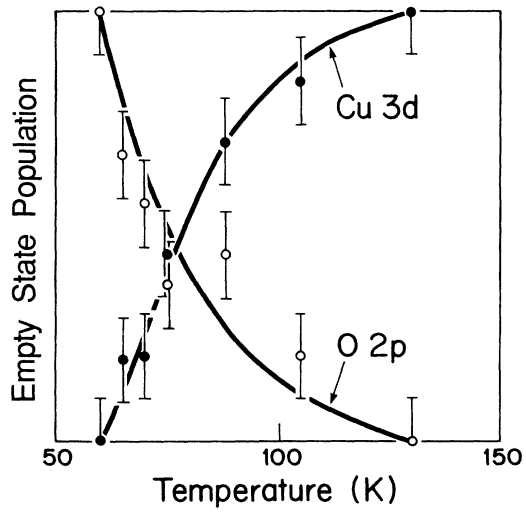

FIG. 5. Increase in O $2p$ holes (open circles) and decrease in Cu $3d$ levels (solid circles) as a function of temperature.

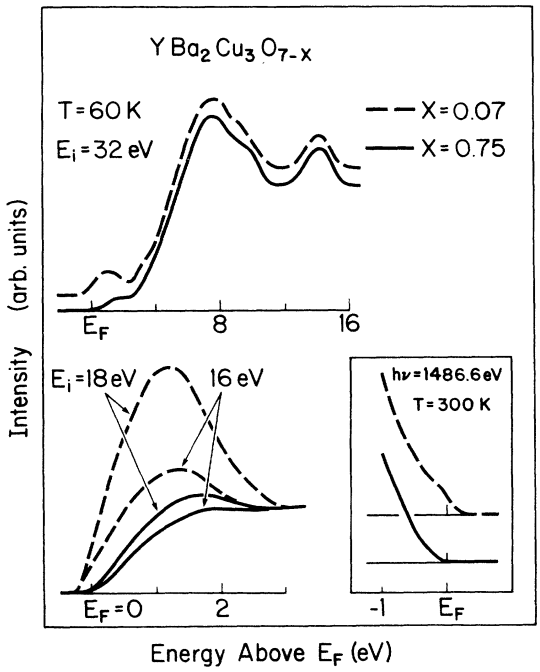

FIG. 6. PDC's for O-rich ($x=0.07$) and O-deficient ($x=0.75$) $YBa_2Cu_3O_{7-x}$ measured at 60 K. In the top panel we present spectra taken at $E_i=32$ eV, while the lower panel shows spectra for $E_i=16$ and 18 eV. The most significant differences were evident within 2 eV of E_F, where there is a large reduction in the O $2p$ hole states for O-deficient samples and there is only a small O $2s$-$2p$ hole resonance. The XPS results shown in the inset reveal a distinct Fermi-level onset for the oxygen-rich sample but no emission at E_F for the oxygen-deficient sample.

O-deficient $YBa_2Cu_3O_{7-x}$

It is well known that the superconducting transition temperature of $YBa_2Cu_3O_{7-x}$ depends on oxygen stoichiometry. It is 93 K for $x<0.25$ (Ref. 54), but drops to 60 K for $0.25<x<0.5$ and to ~ 25 K for $0.5\leq x\leq 0.7$. For $x>0.7$, $YBa_2Cu_3O_{7-x}$ is an antiferromagnetic insulator.[55] With this in mind, we undertook resonant IPES studies of $YBa_2Cu_3O_{6.93}$ and $YBa_2Cu_3O_{6.25}$, to investigate changes in the O $2p$ hole population above E_F.

In Fig. 6 we present spectra for oxygen-rich (dashed line, $x=0.07$) and oxygen-deficient (solid line, $x=0.75$) $YBa_2Cu_3O_{7-x}$. All spectra were acquired within ~ 1 h of fracturing at 60 K. In general, the two $E_i=32$-eV spectra shown in the top panel of Fig. 6 are very similar, except for the reduced emission near E_F for the oxygen-

deficient sample. The Ba 5*d* levels are centered at E_F+7 eV, as determined by the resonance at this energy when E_i was scanned through the Ba 5*p*-5*d* giant dipole resonant transition.[19,50] Likewise, the Y 4*d* character of the structure at E_F+9 eV can be identified because it is enhanced at the Y 4*p*-4*d* giant dipole resonance. The Ba 4*f* levels appear at E_F+14 eV, and they become more pronounced at higher E_i's because of the cross section of $l=3$ states.[50] These Ba 4*f* levels are shifted away from E_F by 4.7 eV compared to Ba metal, a signature of the highly ionic environment of Ba in the oxide superconductor. As shown, the shape and energy position of the unoccupied Y 4*d* and Ba 5*d* manifold remains essentially unchanged for superconducting and nonsuperconducting Y-Ba-Cu-O, and there is no energy shift found for the localized Ba 4*f* levels. This is not surprising since the Cu-O chains and planes are most affected by the removal of oxygen.[56]

In the lower left panel of Fig. 6, we show IPES spectra on and below the O 2*s*-2*p* resonance, normalized to the emission intensity at E_F+3 eV. For $x=0.75$, they show no emission at E_F, and there is significant reduction in emission to E_F+2 eV. There is also a drastic reduction in the O 2*p* hole resonance for O-deficient samples. These changes near E_F are consistent with oxygen loss from Cu-O chains and planes for $x<1$,[56] and conversion from metallic to nonmetallic state.[40] A similar reduction in O 2*p* holes near E_F has been observed in recent energy-loss results near the O 1*s* threshold for O-deficient samples.[10,15]

The inset of Fig. 6 shows the emission for the occupied states within 1 eV of E_F for these $x=0.07$ and 0.75 Y-Ba-Cu-O samples. These XPS (Ref. 57) results reveal a large reduction in emission at E_F for $x=0.75$, in agreement with results by Arko *et al.*[43] and the IPES results. Note that they also show a distinct Fermi-level step for oxygen-rich samples prepared at 300 K. It is then clear that the depletion of O in the Cu-O structures can be readily observed by changes in the electronic states on either side of E_F.

Nonsuperconducting $PrBa_2Cu_3O_{7-x}$

The $RBa_2Cu_3O_7$ composites exhibit superconducting transitions near 90 K for $R=$Y, La, Nd, Sm, Eu, Gd, Ho, Er, and Lu.[58] For Tb and Ce, the 1:2:3 compound does not form, but a stable, nonsuperconducting Pr-Ba-Cu-O compound does exist. Initial speculation concerning the absence of superconductivity for Pr-Ba-Cu-O was that charge from tetravalent Pr atoms would saturate the O 2*p* holes and quench superconductivity. However, resonant photoemission and BIS results suggested that Pr is near a 3+ valence state,[59,60] and x-ray absorption measurements showed a Pr valence of 3.1.[61] Therefore, while the formal valence of Pr appeared to be slightly higher than Y, there was no evidence that the O 2*p* holes were saturated. The present measurements with IPES directly determine the effect of Pr substitution for Y in terms of the O 2*p* holes.

In the top panel of Fig. 7 we compare $E_i=32$-eV spectra for Y-Ba-Cu-O (dashed curves) and Pr-Ba-Cu-O (solid curves). Even though there is the loss of photon emission at E_F for the Pr-Ba-Cu-O sample, a change which will be discussed in detail later, we find no changes in the position or width of the corelike Ba 4*f* levels. Furthermore, we find no significant changes in the Ba 5*d* emission, as judged from IPES measurements for E_i in the range of the Ba 5*p*-5*d* giant dipole enhancement. These results suggest that the Ba atomic environment is not altered by the replacement of Y with Pr.

The substitution of Pr for Y removes the Y 4*d* levels at E_F+9 eV but adds Pr 5*d*- and 4*f*-derived levels. The unoccupied Pr 5*d* levels are centered near E_F+8 eV, as determined by E_i-dependent studies and the use of the Pr 5*p*-5*d* giant dipole resonance at $E_i\sim41$ eV. Much more difficult to place are the many multiplet levels associated with the 4*f*'s of Pr.[59] BIS studies by Kang *et al.*[59] have shown these unoccupied Pr 4*f* levels to extend from near E_F to ~12 eV above E_F in Pr-Ba-Cu-O. Close comparison of the Y-Ba-Cu-O and Pr-Ba-Cu-O spectra does show small Pr 4*f* contributions near $E_F+1.5$ eV and an overall broadening of the Ba and Pr 5*d* manifold as a result of the broad Pr 4*f* peak centered ~7 eV above E_F (FWHM of ~4.5 eV).[59] The absence of distinct features

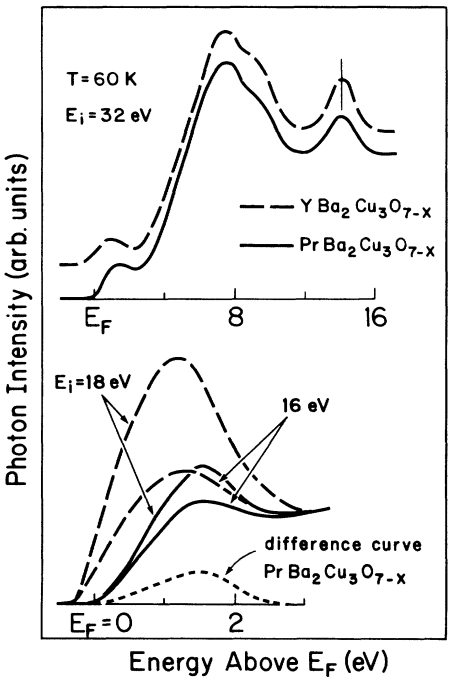

FIG. 7. IPES spectra displaying differences between nonsuperconducting Pr-Ba-Cu-O (solid line) and oxygen-rich Y-Ba-Cu-O (dashed line). The bottom curves show spectra acquired at $E_i=16$ and 18 eV. Substitution of Pr for Y does not eliminate empty-state O 2*p* character, as is evident by the persistence of the O 2*p* hole resonance. However, there are large losses at E_F, and the center of the O 2*p* levels is shifted to ~1.5 eV above E_F. The top curves taken at $E_i=32$ eV show similar structure for Pr-Ba-Cu-O and Y-Ba-Cu-O, with only minor changes attributed to Pr substitution. The position of the corelike Ba 4*f* levels remains constant relative to E_F, even though we observe the formation of a semiconducting gap for Pr-Ba-Cu-O.

at IPES energies is not surprising because of the multiplet splittings, the low concentration of Pr, and the low photoionization cross section of f levels at $E_i = 32$ eV.

In the bottom panel of Fig. 7 we present spectra taken at and below the O 2s-2p resonance. They are normalized to photon emission intensity at $E_F + 3$ eV. Results of Y-Ba-Cu-O are shown for comparison. The difference curve for Pr-Ba-Cu-O (dotted line) again highlights the distribution of O 2p hole character. As shown, there is reduced emission at E_F. The O 2p hole resonance for Pr-Ba-Cu-O is greatly reduced but it is still twice as strong as that for oxygen-deficient Y-Ba-Cu-O. It is also shifted to ~ 1.5 eV above E_F. EELS results by Nucker *et al.*[17] show similar reduction and shifts in the O 2p hole states for the Pr-substituted perovskite. Both studies demonstrate the persistence of empty states with O 2p character. Since the number of O 2p holes is reduced, it is possible that the valency of Pr is greater than 3+, but there is no evidence that it is close to 4+, in agreement with the results by Kang *et al.*[59] and Horn *et al.*[61]

Effects of high-energy electron bombardment

BIS measurements on Y-Ba-Cu-O were performed to obtain insight into the distribution of empty Cu 3d-derived states. With x-ray energies, we tried to enhance the unoccupied Cu 3d cross section, as was possible for CuO. For BIS, the current to the sample was ~ 100 μA (irradiated surface area of 1×5 mm) and the sample temperature rose from 60 to 90 K. The result was that exposure to the beam of ~ 1500-eV electrons led to significant changes in the surface, as judged by surface-sensitive nondisruptive ultraviolet IPES measurements ($E_i \sim 20$-eV power levels 10^{-3} times that of BIS).

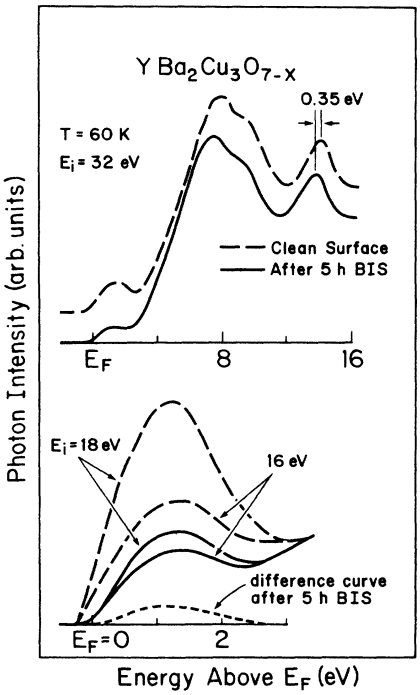

FIG. 8. IPES spectra taken before and after ~ 5 h of exposure to a 1500-eV electron beam (beam size 1×5 mm, current through sample ~ 100 μA). The top panel shows loss of emission at E_F and an ~ 0.35-eV shift toward E_F for the beam-damaged surface. The bottom panel shows a large reduction in the number of O 2p hole states for the beam-altered surface.

The IPES spectra in Fig. 8 show the effects of BIS on Y-Ba-Cu-O for $x = 0.07$ as measured with $E_i = 32$ eV (top) and 16 and 18 eV (bottom). The dashed curves were observed for the freshly fractured sample at 60 K. The solid lines represent data taken after ~ 5 h exposure to the 1500-eV electron beam. They show a large reduction in emission near E_F and a rigid 0.35-eV shift toward E_F of the spectrum following BIS. This shift is most clearly evident from the corelike Ba 4f emission located at $E_F + 14$ eV for the clean surface but 13.65 eV for the BIS-altered surface. Despite the shift, the spectral shape did not change significantly. The difference curve shown in Fig. 8 was obtained by subtracting the 16-eV spectrum from the 18-eV spectrum for the electron-beam-damaged surface. Again, there is a reduction in emission near E_F for both $E_i = 16$ and 18 eV because of electron irridation and an 80% reduction in the O 2p hole resonance.

We also investigated the stability of Bi-Sr-Ca-Cu-O to high-energy electron bombardment at 60 K. Our results indicate that the O 2p hole resonance is reduced by $\sim 20\%$ after 5 h and $\sim 40\%$ after 10 h of BIS (same electron flux as for Y-Ba-Cu-O). No shifts in the unoccupied electronic structure were observed. We conclude that, even though one should be careful when using high-energy electron probes on Bi-Sr-Ca-Cu-O, the effects are much less severe than with Y-Ba-Cu-O.

Modifications by Au and Cu adatoms on Y-Ba-Cu-O and Bi-Sr-Ca-Cu-O

The properties of metal- and semiconductor-superconductor interfaces formed at 300 K have been studied in detail over the past several years.[25,62–66] Those results demonstrated that elements with a high affinity toward oxide formation (e.g., Ti, Al, Fe, Cu, and Ge) leech oxygen from the surface region of the ceramic to form oxides in the interface region.[25,62–63] Ultimately, the removal of oxygen from the substrate becomes kinetically limited, and an elemental overlayer forms. In contrast Au, Ag, CaF_2, BiO, and Al_2O_3 show no tendency to remove oxygen from the substrate, but deposition is accompanied by varying degrees of substrate disruption.[64,65] Here, we are interested in investigating the effects of Cu and Au deposition at 60 and 300 K in the context of the O 2p holes.

Figure 9 shows representative IPES spectra for Cu overlayer growth on Y-Ba-Cu-O (top) and Bi-Sr-Ca-Cu-O (bottom) at 60 K for different amounts of metal θ. Corresponding results for Au are shown in Fig. 10. The $\theta = 0$ curves are for the clean surface. The solid lines represent off-resonance spectra, $E_i = 16$ eV, and the dashed lines show on-resonance spectra, $E_i = 18$ eV. They have been normalized at $E_F + 3$ eV and overlap at higher energy. Equivalent results were obtained at 300 K when account

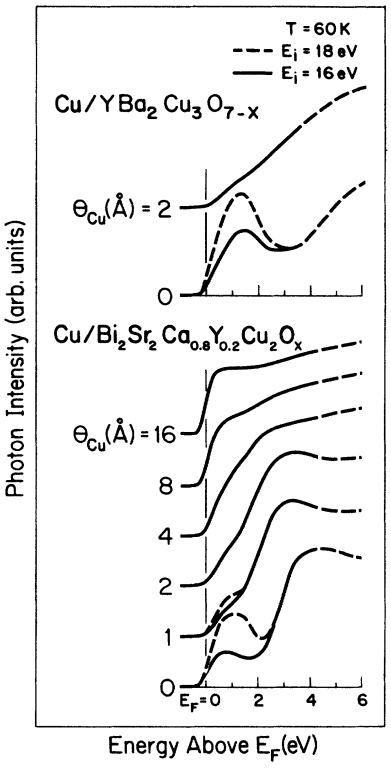

FIG. 9. IPES spectra showing interface formation for Cu/Y-Ba-Cu-O (top) and Cu/Bi-Sr-Ca-Cu-O (bottom). Dashed curves represent spectra taken at $E_i = 18$ eV and solid lines are for $E_i = 16$ eV. Measurements and evaporations were done at 60 K. Cu adatoms quench the O 2p hole state resonance by $\theta_{Cu} = 2$ Å for both substrates, producing a nonsuperconducting surface region.

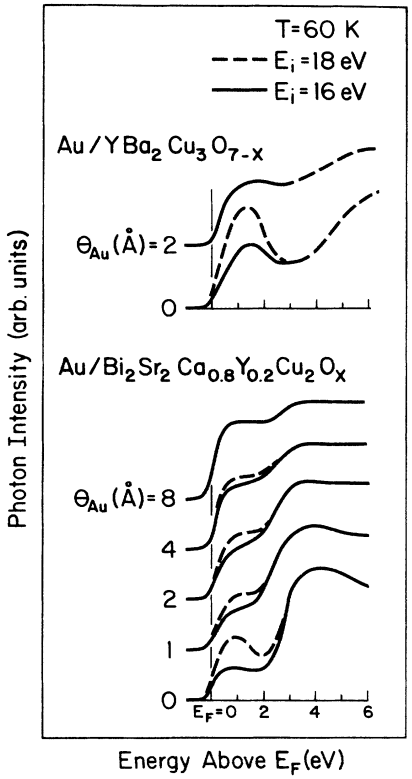

FIG. 10. IPES spectra showing interface formation for Au/Y-Ba-Cu-O and Au/Bi-Sr-Ca-Cu-O, as in Fig. 9. Au deposition on Y-Ba-Cu-O led to disruption and reduced O 2p hole resonance by 2 Å. The persistence of this resonance past 4 Å for Bi-Sr-Ca-Cu-O suggests that the Bi-Sr-Ca-Cu-O surface is more stable.

is taken of temperature dependent O 2p population discussed earlier. As shown, the deposition of 2 Å of Cu (Fig. 9) produces a surface region where the O 2p hole states are missing from both Y-Ba-Cu-O and Bi-Sr-Ca-Cu-O. This is evident by the large reduction in emission near E_F, and the loss of O 2s-2p resonant enhancement. The significance of these results is that all O 2p hole states characteristic of the superconductor are destroyed within the probe depth of IPES ($3\lambda = 12$ Å). Moreover, the interface region is no longer conducting since there is no emission at E_F until $\theta_{Cu} = 8$ Å when metallic Cu starts to form over the disrupted region. These empty-state results complement those obtained with XPS that showed dramatic loss of the Cu $2p_{3/2}$ satellite that is indicative of formal 2+ valence.[62] The XPS results make it possible to conclude that nearly all of the Cu atoms within ~50 Å of the surface have undergone a valence change from 2+ or 1+ as Cu adatoms react with oxygen from the superconductor and destroy the structure of the surface region.

The results of Fig. 10 show that Au overlayers also modify the Y-Ba-Cu-O and Bi-Sr-Ca-Cu-O surfaces. For Y-Ba-Cu-O, 2 Å of Au quenches the O 2p hole resonant enhancement within our 12 Å probe depth, demonstrating that at least the topmost ~10 Å of the surface is vulnerable to adatom-induced structural modification. For Bi-Sr-Ca-Cu-O, the effect is much less, as shown by the persistence of O 2p hole state enhancement past 4 Å. For Bi-Sr-Ca-Cu-O, we estimate that only the topmost ~5 Å of the substrate are disrupted (although it should be noted that we cannot comment on the lateral homogeneity of the disruption). These results are also in agreement with XPS results[64] which showed Y-Ba-Cu-O to be much more susceptible to surface disruption than Bi-Sr-Ca-Cu-O.

During interface development for Y-Ba-Cu-O, we also monitored the empty corelike Ba 4f level.[50] For Cu deposition, the Ba 4f structure shifted and broadened from its clean surface position of 14 (FWHM = 2.2 eV) to 12.9 eV (FWHM = 3.4 eV). This provides additional evidence that changes occur in the surface region that alter the chemical environment of all of the constituents, producing a highly disrupted region bearing little resemblance to the perovskite structure. In contrast, for Au the Ba 4f emission shifted from 14 (FWHM = 2.2 eV) to 13.8 eV (FWHM = 2.4 eV), an amount equal to that observed in XPS studies of Au and Ag overlayers during the first angstroms of deposition.[64] Since all of the electronic states move in registry, the origin is probably electrostatic in nature, i.e., because of rigid shifts of E_F as rehybridization alters the distribution of states near E_F.

CONCLUSIONS

This paper has focused on the oxygen 2*p* holes in the high-temperature superconductors. We have shown that these empty states can be highlighted by energy-dependent inverse photoemission in the vicinity of the O 2*s*-2*p* resonance. Temperature-dependent IPES results have shown that the amount of O 2*p* hole emission increases substantially as the temperature is reduced from 300 to 60 K for both Y-Ba-Cu-O and Bi-Sr-Ca-Cu-O. We also observe changes in the Cu-derived empty states, and the variation in Cu- and O-derived features indicates a buildup in the number of O holes and increased Cu valence at low temperature. There is no evidence for temperature changes in states unrelated to the CuO_2 planes. Studies of oxygen-rich and oxygen-deficient Y-Ba-Cu-O showed the disappearance of O 2*p* holes above E_F, in agreement with EELS studies, absorption measurements, and direct photoemission measurements. Intriguingly, results for nonsuperconducting Pr-Ba-Cu-O also showed O 2*p* holes above E_F, but they are found to be reduced and altered. [Superconductivity is quenched for $y=0.1$ in $EuBa_2(Cu_{1-y}Zn_y)_3O_7$, but absorption studies by den Boer *et al.*[11] found no reduction in O 2*p* holes from $y=0.0$ to 0.1.] Evidently, the presence of O 2*p* empty-state character does not guarantee superconductivity, but their absence is sufficient to suppress the high-T_c mechanism.

Finally, we showed the O 2*p* holes to be very sensitive to surface disruptions. We found evidence for surface disruption of the uppermost CuO_2 plane for Y-Ba-Cu-O at 300 K. Furthermore, high-energy electron bombardment at 60 K was also shown to disrupt the Y-Ba-Cu-O surface. Disruption of Bi-Sr-Ca-Cu-O was much smaller. Finally, Cu and Au adatoms were found to react and disrupt the surfaces of Y-Ba-Cu-O and Bi-Sr-Ca-Cu-O, and the results were independent of temperature in the range 60–300 K. The disruption was found to be larger for Y-Ba-Cu-O, in agreement with previous accounts of the stability of the Y-Ba-Cu-O surface.

ACKNOWLEDGMENTS

The work at the University of Minnesota was supported by the Office of Naval Research and U.S. Defense Advanced Research Projects Agency (DARPA) under Contract Nos. (ONR) N00014-87-K-0029 and N00014-88-K-0637. That at Argonne National Laboratory was supported by the Department of Energy, Office of Basic Energy Sciences and Materials Science. The authors thank C. G. Olson, A. J. Arko, W. E. Pickett, and C. R. Brundle for making their results available prior to publication.

[1]M. W. Shafer, T. Penney, and B. L. Olson, Phys. Rev. B **36**, 4047 (1987).

[2]H. Takagi, H. Eisaki, S. Uchida, A. Maeda, S. Tajima, K. Uchinokura, and S. Tanaka, Nature (London) **332**, 236 (1988).

[3]V. J. Emery, Phys. Rev. Lett. **58**, 2794 (1987).

[4]F. C. Zhang and T. M. Rice, Phys. Rev. B **37**, 3759 (1988).

[5]D. D. Sarma, S. Ramasesha, and A. Taraphder, Phys. Rev. B **39**, 12286 (1989).

[6]M. F. Hundley, A. Zettl, A. Stacy, and M. L. Cohen, Phys. Rev. B **35**, 8800 (1987).

[7]N. P. Ong, Z. Z. Wang, J. Clayhold, J. M. Tarascon, L. H. Green, and W. R.McKinnon, Phys. Rev. B **35**, 8807 (1987).

[8]J. A. Yarmoff, D. C. Clarke, W. Drube, U. O. Karlsson, A. Taleb-Ibrahimi, and F. J. Himpsel, Phys. Rev. B **36**, 3967 (1987).

[9]D. Sondericker, Z. Fu, D. C. Johnston, and W. Eberhardt, Phys. Rev. B **36**, 3983 (1987).

[10]P. Kuiper, G.Kruizinga, J. Ghijsen, M. Grioni, P. J. W. Weijs, F. M. F. de Groot, G. A. Sawatzky, H. Verweij, L. F. Feiner, and H. Petersen, Phys. Rev. B **38**, 6483 (1988).

[11]M. L. denBoer, C. L. Chang, H. Petersen, M. Schaible, K. Reilly, and S. Horn, Phys. Rev. B **38**, 6588 (1988).

[12]F. J. Himpsel, G. V. Chandrashekhar, A. B. McLean, and M. W. Shafer, Phys. Rev. B **38**, 11 946 (1988).

[13]N. Nucker, J. Fink, B. Renker, D. Ewert, C. Politis, P. J. W. Weijs, and J. C. Fuggle, Z. Phys. B **67**, 9 (1987).

[14]P. E. Batson and M. F. Chisholm, Phys. Rev. B **37**, 635 (1988).

[15]N. Nucker, J. Fink, J. C. Fuggle, P. J. Durham, and W. M. Temmerman, Phys. Rev. B **37**, 5158 (1988).

[16]N. Nucker, H. Romberg, X. X. Xi, J. Fink, B. Gegenheimer, and Z. X. Zhao, Phys. Rev. B **39**, 6619 (1989).

[17]N. Nucker, J. Fink, J. C. Fugglè, P. J. Durham, and W. M. Temmerman, Physica C **153-155**, 119 (1988).

[18]T. J. Wagener, Yongjun Hu, Y. Gao, M. B. Jost, J. H. Weaver, N. D. Spencer, and K. C. Goretta, Phys. Rev. B **39**, 2928 (1989).

[19]H. M. Meyer III, T. J. Wagener, J. H. Weaver, and D. S. Ginley, Phys. Rev. B **39**, 7343 (1989).

[20]W. Drube, F. J. Himpsel, G. V. Chandrashekhar, and M. W. Shafer, Phys. Rev. B **39**, 7328 (1989).

[21]G. Wendin, J. Phys. (Paris) **48**, C9-1157 (1988).

[22]Y. Gao, M. Grioni, B. Smandek, J. H. Weaver, and T. Tyrie, J. Phys. E **21**, 489 (1988).

[23]J. H. Weaver, H. M. Meyer III, T. J. Wagener, D. M. Hill, and Yongjun Hu, in *High-T_c Superconducting Thin Films, Devices, and Applications,* Proceedings of the 1988 Topical Conference on High T_c Superconducting Thin Films, Devices, and Applications of the AVS, Atlanta, GA, 1988, AIP Conf. Proc. No. 182, edited by Giorgio Margaritondo, Robert Joynt, and Marshall Onellion (AIP, New York, 1989); H. M. Meyer III, T. J. Wagener, J. H. Weaver, and D. S. Ginley, Phys. Rev. B **39**, 7343 (1989).

[24]T. J. Wagener, H. M. Meyer III, D. M. Hill, Yongjun Hu, M. B. Jost, J. H. Weaver, D. Hinks, B. Dabrowski, and D. R. Richards, Phys. Rev. B **40**, 4532 (1989).

[25]H. M. Meyer III, D. M. Hill, T. J. Wagener, Y. Gao, J. H. Weaver, D. W. Capone II, and K. C. Goretta, Phys. Rev. B **38**, 6500 (1988).

[26]K. C. Goretta, I. Bloom, Nan Chen, G. T. Goudey, M. C. Hash, G. Klassen, M. T. Lanagan, R. B. Poeppel, J. P. Singh, Donglu Shi, U. Balachandran, J. T. Dusek, and D. W. Capone II, Mater. Lett. **7**, 161 (1988).

[27]U. Balachandran (unpublished).
[28]N. Uno, N. Enomoto, Y. Tanaka, and H. Takami, Jpn. J. Appl. Phys. **27**, L1003 (1988).
[29]P. K. Gallagher, Adv. Ceram. Mater. **2**, 632 (1987).
[30]K. Kishio *et al.*, Jpn. J. Appl. Phys. **26**, L1228 (1987).
[31]J. Ghijsen, L. H. Tjeng, J. van Elp. H. Eskes, J. Westerink, G. A. Sawatzky, and M. T. Czyzyk, Phys. Rev. B **38**, 11 332 (1988).
[32]M. Grioni, M. T. Czyzyk, F. M. F. de Groot, J. C. Fuggle, and B. E. Watts, Phys. Rev. B **39**, 4886 (1989).
[33]S. Åsbrink and L.-J. Norrby, Acta Crystallogr. Sect. B **26**, 8 (1970).
[34]F. P. Koffyberg and F. A. Benko, J. Appl. Phys. **53**, 1173 (1982).
[35]M. R. Thuler, R. L. Benbow, and Z. Hurych, Phys. Rev. B **26**, 669 (1982).
[36]Th. Fauster and F. J. Himpsel, Phys. Rev. B **30**, 1874 (1984).
[37]J. J. Yeh and I. Lindau, in At. Data Nucl. Data Tables **32**, 1 (1985).
[38]G. A. Sawatzky and J. W. Allen, Phys. Rev. Lett. **53**, 2339 (1984).
[39]W. Drube and F. J. Himpsel, Phys. Rev. Lett. **60**, 140 (1988).
[40]W. E. Pickett, Rev. Mod. Phys. **61**, 433 (1989), and detailed references therein.
[41]L. F. Mattheiss and D. R. Hamann, Phys. Rev. Lett. **60**, 2681 (1988); B. A. Richert and R. W. Allen (unpublished).
[42]W. Drube, D. Straub, and F. J. Himpsel, Phys. Rev. B **35**, 5563 (1987).
[43]A. J. Arko, R. S. List, R. J. Bartlett, S-W. Cheong, Z. Fisk, J. D. Thompson, C. G. Olson, A-B. Yang, R. Liu, C. Gu, B. W. Veal, J. Z. Liu, A. P. Paulikas, K. Vandervoort, H. Clasus, J. C. Campuzano, J. E. Schirber, and N. D. Shinn, Phys. Rev. B **40**, 2268 (1989).
[44]T. J. Wagener, Yongjun Hu, M. B. Jost, J. H. Weaver, and C. Gallo (unpublished).
[45]U. Fano, Phys. Rev. **124**, 1866 (1961).
[46]T. Takahashi, H. Matsuyama, H. Katayama-Yoshida, Y. Okabe, S. Hosoya, K. Seki, H. Fujimoto, M. Sato, and H. Inokuchi, Nature (London) **334**, 691 (1988).
[47]J.-M. Imer, F. Patthey, B. Dardel, W.-D. Schneider, Y. Baer, Y. Petroff, and A. Zettl, Phys. Rev. Lett. **62**, 336 (1989).
[48]Y. Chang, Ming Tang, R. Zanoni, M. Onellion, Robert Joynt, D. L. Huber, G. Margaritondo, P. A. Morris, W. A. Bonner, J. M. Tarascon, and N. G. Stoffel, Phys. Rev. B **39**, 4740 (1989).
[49]C. G. Olson, R. Liu, A.-B. Yang, D. W. Lynch, A. J. Arko, R. S. List, B. W. Veal, Y. C. Chang, P. Z. Jiang, and A. P. Paulikas, Science **245**, 731 (1989).
[50]T. J. Wagener, Y. Gao, J. H. Weaver, A. J. Arko, B. Flandermeyer, and D. W. Capone II, Phys. Rev. B **36**, 3899 (1987).
[51]D. D. Sarma and C. N. R. Rao, J. Phys. C **20**, L659 (1987).
[52]It is doubtful that this increase is caused by chemisorbed oxygen, since we showed that this feature appears at ~ 1.8 eV above E_F with a FWHM of ~ 2 eV, and it did not become significant until after ~ 4 h (1×10^{-10} Torr) (Ref. 50).
[53]Z.-X. Shen, P. A. P. Lindberg, D. S. Dessau, I. Lindau, W. E. Spicer, D. B. Mitzi, I. Bozovic, and A. Kapitulnik, Phys. Rev. B **39**, 4295 (1989).
[54]R. J. Cava, B. Batlogg, C. H. Chen, E. A. Rietman, S. M. Zahurak, and D. Werder, Phys. Rev. B **36**, 5719 (1987).
[55]J. H. Brewer *et al.*, Phys. Rev. Lett. **60**, 1073 (1988).
[56]J. Zaanen, A. T. Paxton, O. Jepsen, and O. K. Anderson, Phys. Rev. Lett. **60**, 2685 (1988).
[57]H. M. Meyer III, T. J. Wagener, and J. H. Weaver (unpublished).
[58]P. H. Hor, R. L. Meng, Y. Q. Wang, L. Gao, Z. J. Huang, J. Bechtold, K. Forster, and C. W. Chu, Phys. Rev. Lett. **58**, 1891 (1987).
[59]J.-S. Kang, J. W. Allen, Z.-X. Shen, W. P. Ellis, J. J. Yeh, B. W. Lee, M. B. Maple, W. E. Spicer, and I. Lindau, J. Less-Common Met. **148**, 121 (1989).
[60]J. H. Weaver, H. M. Meyer III, T. J. Wagener, D. M. Hill, Y. Gao, D. Peterson, Z. Fisk, and A. J. Arko, Phys. Rev. B **38**, 4668 (1988).
[61]S. Horn, J. Cai, S. A. Shaheen, Y. Jeon, M. Croft, C. L. Chang, and M. L. denBoer, Phys. Rev. B **36**, 3895 (1987).
[62]D. M. Hill, H. M. Meyer III, J. H. Weaver, C. F. Gallo, and K. C. Goretta, Phys. Rev. B **38**, 11331 (1989).
[63]Y. Gao, H. M. Meyer III, T. J. Wagener, D. M. Hill, S. G. Anderson, J. H. Weaver, B. Flandermeyer, and D. W. Capone II, in *Thin Film Processing and Characterization of High Temperature Superconductors*, Proceedings of the American Vacuum Society Topical Conference on Thin Film Processing and Characterization of High-T_c Superconductors, AIP Conf. Proc. No. 165, edited by J. M. E. Harper, R. J. Colton, and L. C. Feldman (AIP, New York, 1988).
[64]H. M. Meyer III, D. M. Hill, T. J. Wagener, J. H. Weaver, C. F. Gallo, and K. C. Goretta, J. Appl. Phys. **65**, 3130 (1989).
[65]D. M. Hill, H. M. Meyer III, J. H. Weaver, and D. L. Nelson, Appl. Phys. Lett. **53**, 1657 (1988).
[66]P. A. P. Lindberg, Z.-X. Shen, I. Lindau, W. E. Spicer, C. B. Eom, and T. H. Geballe, Appl. Phys. Lett. **53**, 529 (1988).